Title
Stable Gene Silencing in Zebrafish with Spatiotemporally Targetable RNA Interference

Journal
Genetics, 193(4)

ISSN
0016-6731

Authors
Dong, Zhiqiang
Peng, Jisong
Guo, Su

Publication Date
2013-04-01

DOI
10.1534/genetics.112.147892

Peer reviewed

Stable Gene Silencing in Zebrafish with Spatiotemporally Targetable RNA Interference

Zhiqiang Dong,[1] Jisong Peng,[1] and Su Guo[2]
Department of Bioengineering and Therapeutic Sciences, Programs in Human Genetics and Biological Sciences, University of California, San Francisco, California 94143-2811

ABSTRACT The ability to regulate gene activity in a spatiotemporally controllable manner is vital for biological discovery that will impact disease diagnosis and treatment. While conditional gene silencing is possible in other genetic model organisms, this technology is largely unavailable in zebrafish, an important vertebrate model organism for functional gene discovery. Here, using short hairpin RNAs (shRNAs) designed in the microRNA-30 backbone, which have been shown to mimic natural microRNA primary transcripts and be more effective than simple shRNAs, we report stable RNA interference-mediated gene silencing in zebrafish employing the yeast Gal4-UAS system. Using this approach, we reveal at single-cell resolution the role of atypical protein kinase Cλ (aPKCλ) in regulating neural progenitor/stem cell division. We also show effective silencing of the *one-eyed-pinhead* and *no-tail/brachyury* genes. Furthermore, we demonstrate stable integration and germ-line transmission of the UAS-miR-shRNAs for *aPKCλ*, the expressivity of which is controllable by the strength and expression of Gal4. This technology shall significantly advance the utility of zebrafish for understanding fundamental vertebrate biology and for the identification and evaluation of important therapeutic targets.

STUDIES of genetic model organisms contribute tremendously to our understanding of diverse biological processes and human disorders at molecular and cellular levels (Davis 2004; Aitman *et al.* 2011). As a recently established animal model, zebrafish has salient features that promise to provide new insights into biology and medicine. These include rapid external development, transparent embryonic and larval stages, simpler vertebrate organ systems, and amenability for genetic and chemical screening. The utility of zebrafish, however, has been hampered by the inability to silence genes in a spatiotemporally controllable manner. Although valuable reverse genetic methods are available (Nasevicius and Ekker 2000; Wienholds *et al.* 2002; Doyon *et al.* 2008; Meng *et al.* 2008; Huang *et al.* 2011; Sander *et al.* 2011; Bedell *et al.* 2012), none offer gene silencing at any desired stages of the life cycle and in any cell types of interest.

doi: 10.1534/genetics.112.147892
Manuscript received November 21, 2012; accepted for publication January 12, 2013
Supporting information is available online at http://www.genetics.org/lookup/suppl/doi:10.1534/genetics.112.147892/-/DC1.
[1]These authors contributed equally to this work.
[2]Corresponding author: Department of Bioengineering and Therapeutic Sciences, Programs in Human Genetics and Biological Sciences, University of California, San Francisco, CA 94143-2811. E-mail: su.guo@ucsf.edu

RNA interference (RNAi) is a powerful approach to dissect gene function (Fire 2007; Mello 2007). It was originally discovered in *Caenorhabditis elegans*, where the observation of gene inactivation by both sense and antisense RNAs (Guo and Kemphues 1995) led to the finding of double-stranded RNA (dsRNA)-mediated gene silencing (Fire *et al.* 1998). In vertebrates, the effectiveness of RNAi was hindered by the dsRNA-induced interferon response causing nonspecific effects (Manche *et al.* 1992; Stark *et al.* 1998) until the finding of efficacious small interfering RNAs (siRNAs) (Elbashir *et al.* 2001). However, their delivery into zebrafish remains either ineffective or has nonspecific effects (Gruber *et al.* 2005; Zhao *et al.* 2008). Likewise, simple short hairpin RNAs (shRNAs) driven by RNA polymerase III promoters (Paddison *et al.* 2002) also appears ineffective in zebrafish (Wang *et al.* 2010).

Micro-RNAs (miRNAs) are endogenous ~21- to 23-nucleotide RNAs that can regulate gene expression. Originally discovered in *C. elegans* (Lee *et al.* 1993; Reinhart *et al.* 2000), they were later found conserved across animals and plants (Bartel 2009; Ebert and Sharp 2012). The observation that designed miRNAs can inhibit cognate mRNA expression in human cells (Zeng *et al.* 2002) has paved the way for recent developments of shRNAs employing the primary miR-30 backbones (miR-shRNAs) (Dickins *et al.* 2005; Silva *et al.* 2005). This natural configuration is reported 12 times more

efficient than simple hairpin designs. MiR-shRNAs are recently shown to be effective *in vivo* in mice (Dickins *et al.* 2005; Premsrirut *et al.* 2011; Zuber *et al.* 2011) and zebrafish (Dong *et al.* 2009; De Rienzo *et al.* 2012). However, the capability of germ-line transmission is only reported by one study in zebrafish (Dong *et al.* 2009), where functional efficacy and specificity of silencing were not quantitatively documented. Therefore, the potential of RNAi for stable and conditional gene silencing in zebrafish remains uncertain.

With the goal of achieving spatiotemporal and dosage control of gene silencing, we have exploited the miR-shRNA technology in combination with the bipartite Gal4/upstream activating sequence (UAS) system (Ptashne 1988), which offers excellent versatility for spatiotemporal control together with amplification of gene expression level. Using *atypical protein kinase Cλ* (*apkcλ*), *one-eyed pinhead* (*oep*), and *no tail/brachyury* (*ntl*) as test loci, we show that RNAi in zebrafish is effective, rapid, dosage controllable, stable with conditional capability, and scalable.

Materials and Methods

Zebrafish strains

Wild-type embryos were obtained from natural spawning of AB adults. The transgenic line *Tg[ubi-GFF]* (Asakawa and Kawakami 2010) was a gift from K. Kawakami. The *apkcλ* mutant *heart and soul* was kindly provided by D. Stainier.

ShRNA design

ShRNA design was performed using the siRNA design tool from the following website: http://www.genscript.com/design_center.html, which ranks target candidates based on a proprietary algorithm using ΔE parameters. We further refined the list by removing the candidates that have more than three G/C in 6–11 nt of the target sequences, based on a thermodynamic study of siRNA (Ui-Tei *et al.* 2008).

Vector construction

The shRNA precursor structure was designed based on the miR-30e precursor in zebrafish. The miR-30e target and guide sequences were replaced with the predicted shRNA target and guide sequences. To best mimic the miR-30e precursor structure, we kept the original loop region and the flanking sequences of the miR-30e precursor and introduced two mismatched "TT" into the shRNA guide sequence between nt 12 and nt 13. We synthesized a pair of complementary oligos that include all the designed shRNA structures (guide sequence, loop sequence, target sequence, and the flanking sequences) and the annealed oligos were inserted into zebrafish miR-30e backbone in expression vectors kindly provided by the late Ting Xi Liu (Dong *et al.* 2009). The following *5xUAS* sequence was used: *cggagtactg tcctccgagcggagtactgtcctccgagcggagtactgtcctccgagcggagtactgtcct ccgagcggagtactgtcctccg*.

DNA and RNA injection

DNA and RNA injections were performed at the one-cell stage. For genetic mosaic analyses, RNAi constructs (UAS-TdTomato-shRNA1$^{apkc\lambda}$-miniTol2 or UAS-TdTomato-shRNA5$^{apkc\lambda}$-miniTol2; 75 pg per embryo) were co-injected with EF1α-GFF-PT2KXIG (elongation factor 1a regulatory element-driven Gal4) (50 pg per embryo) and Tol2 tranposase (10 pg per embryo). Sense strand-capped RNA was synthesized by SP6 transcription from *Not*I-linearized plasmid using the mMESSAGE mMACHINE system (Ambion). RNAi-resistant sense RNAs for *apkcλ*, *ντλα ανδ οεπα*, as well as RNAs encoding the *oep*-shRNA and *ntla*-shRNA, were injected at 400 pg per embryo. For time-lapse *in vivo* imaging, 3NLS:EGFP sense RNA (200 pg per embryo) was co-injected with EF1α-GFF-PT2KXIG DNA (50 pg per embryo) and 5xUAS-tdTomato-shRNA$^{apkc\lambda}$ plasmid DNA (75 pg per embryo).

Heat shock of zebrafish embryos

Heat shock of zebrafish embryos was performed at the stage of 8 hours postfertilization (hpf) (75% epiboly). Fertilized embryos were collected from the cross between the *UAS-TdTom-miR-shRNA1$^{apkc\lambda}$* founder A and the *hsp70-Gal4* transgenic animal, and were raised at 28.5° before heat shock. A 500-ml glass beaker filled with 100 ml egg water was preheated to 37° in a water bath right before heat shock. Around 100 embryos were transferred to the preheated egg water at 8 hpf and incubated in a 37° water bath for 1 hr. The embryos were then transferred to 28.5° egg water immediately and raised in a 28.5° incubator until analysis.

Phenotypic analyses

Phenotypic analyses were performed manually under a bright field dissection microscope. For *apkcλ* RNAi, four morphological phenotypes were analyzed, which are typically observed in the *apkcλ* mutant (*heart and soul*) (Horne-Badovinac *et al.* 2001): (1) defect in heart tube assembly, (2) patchy retinal pigmented epithelium, (3) failure of the brain ventricle to inflate, and (4) abnormal body curve. The number of embryos that are positive for each phenotype as well as the total number of all embryos was counted for both RNAi groups and control groups. Statistic analyses were performed based on positive percentage for each phenotype. For *ntla* and *oep* RNAi, the typical no-tail phenotype and one-eyed pinhead phenotype were analyzed.

Time-lapse in vivo imaging

To observe the division orientation of radial glia progenitor cells, time-lapse *in vivo* imaging was performed on embryos injected with 3NLS:EGFP sense RNA, EF1α-GFF-PT2KXIG DNA, and 5xUAS-tdTomato-shRNA$^{apkc\lambda}$-miniTol2 DNA (see *DNA and RNA injection* for detail) at 24 hpf. The imaging was performed as previously described (Dong *et al.* 2012). In brief, embryos were mounted in low melting point agarose and properly placed on a temperature-controlled stage

of the confocal microscope. We used a Nikon C1 spectral confocal microscope with upright objectives. Fluorescently labeled individual neural progenitor cells were imaged for 2 hr with a fixed interval of 90 sec under a ×40 water-dipping objective. The parameters of confocal imaging were determined as sufficient to capture the orientation of cell division, while reducing photobleaching during the imaging period.

Immunohistochemistry

Immunohistochemistry was performed on whole mount embryos as described previously (Guo *et al.* 1999). Embryos were fixed with 4% paraformaldehyde. Embryos older than 60 hpf were treated with proteinase K before incubation in primary antibodies (rabbit anti-aPKC 1:100, Santa Cruz sc-216) at 4° overnight. After four washes with phosphate-buffered saline with 0.1% Tween, 0.5% Triton X-100, and 1% DMSO, the embryos were incubated with Alexa Fluor secondary antibody (1:2000, Invitrogen) at 4° overnight. After wash and glycerol sequential treatment, the embryos were mounted and imaged using Nikon C1 confocal microscope.

Quantitative real-time RT–PCR analyses

For the analyses of knockdown of *apkcλ* expression by transient RNAi, the control or RNAi embryos were collected at 10 hpf and total RNA from pooled embryos (20 embryos per sample for each group) was extracted using Trizol reagent (Invitrogen) followed by treatment with Turbo DNA-free DNase (Ambion). First-strand cDNA was reverse transcribed using oligo-dT primers and Superscript reverse transcriptase (Invitrogen). Real-time PCR amplifications of *apkcλ*, *oep*, *ntla*, and *gapdhs* were carried out with SYBR Green PCR Master Mix (Applied Biosystems). Primers used were:

apkcλ F: 5′-CCCGCACCAAGTCCGGGTAA-3′,
apkcλ R: 5′-GCTGAGAAGAAACGGTGCACGGA-3′;
oep F: 5′-ATGGACTTTTGCATTGCTTCCCACA-3′,
oep R: 5′-AGTGTTCTGAGGGAGCCCGACC-3′;
ntla F: 5′-CCCAGCCATTACTCCCACCGC-3′,
ntla R: 5′-TGGGCCAGGGTTCCCATCCC-3′;
gapdhs F: 5′-ACTCCACTCATGGCCGTTAC-3′,
gapdhs R: 5′-TGAGCTGAGGCCTTCTCAAT-3′.

Droplet digital PCR analyses

For the analyses of knockdown of *apkcλ* expression by stable RNAi transgenesis, the sibling control or RNAi transgenic embryos were collected at 24 hpf and total RNA from single embryos was extracted using Trizol reagent (Invitrogen) followed by treatment with Turbo DNA-free DNase (Ambion). First-strand cDNA was reverse transcribed using oligo-dT primers and Superscript reverse transcriptase (Invitrogen). Droplet Digital PCR amplifications of *apkcλ* and *gapdhs* were carried out with primers and probes carrying fluorophore modifications. The sequences of the primers are the same as used in qRT–PCR analyses. Additionally, FAM-modified *apkcλ* probe (5′-FAM-ATGTGCTCCATGGACAATGACCAGCT-3′) and HEX-modified *gapdhs* probe (5′-HEX-TTCCAGTGCATGAAGCC TGCTGAGAT-3′) were used. Data were analyzed using Quantasoft version 1.2.10.0.

Stable transgenesis

Stable UAS-miR-shRNA$^{apckc\lambda}$ transgenic lines were generated using the Tol2 transposon system as described previously (Suster *et al.* 2009). RNAi constructs (UAS-TdTomato-MiR-shRNA1$^{apkc\lambda}$-miniTol2 or UAS-TdTomato-miR-shRNA5$^{apkc\lambda}$-miniTol2; 50 pg per embryo) together with Tol2 transposase (10 pg per embryo) were injected into one-cell-stage embryos of AB wild-type fish. Injected embryos were raised to adulthood (G0) and screened for germ-line transmission by crossing with Tg[Ubi-GFF] transgenic fish. The germ-line transgenic founders would yield embryos with TdTomato expression, which could be easily distinguished under the epifluorescent microscope. The embryos with ubiquitous TdTomato expression were raised to adulthood (F1), which carry both UAS-$^{apckc\lambda}$ RNAi and Ubi-GFF transgenes. Additionally, UAS-RNAi G0 germ-line founders were crossed with AB wild-type fish. All the progenies were raised to adulthood and genotyped by PCR using TdTomato-specific primers to screen for stable transgenic F1 fish. Stable transgenic F1 were obtained for UAS-TdTomato-shRNA1$^{apckc\lambda}$ and UAS-TdTomato-shRNA5$^{apckc\lambda}$.

Results and Discussion

Conditional miR-shRNA expression system

We designed shRNAs employing the primary miR-30 backbones (hence called miR-shRNAs) (Figure 1A). The fluorescent reporter TdTomato conveniently marked the cells that express the miR-shRNAs. Three genes were used as the test set: (1) The *atypical protein kinase C lambda* (*aPKCλ*), for which a distinct loss-of-function phenotype has been documented in zebrafish. We chose this gene also because its disruption produces a highly specific cellular phenotype, that is, an alteration of spindle rotation in dividing radial glia progenitor cells (Horne-Badovinac *et al.* 2001). (2) The *no tail a* (*ntla*) and (3) *one-eyed pinhead* (*oep*) genes, for which distinct loss-of-function phenotypes can be readily assessed (Schulte-Merker *et al.* 1994; Zhang *et al.* 1998). Using the Web-based shRNA design tool (www.genescript.com) together with the filtering criteria based on thermodynamic properties (Ui-Tei *et al.* 2008), six shRNAs targeting the *apkcλ* gene (Supporting Information, Figure S1), four shRNAs each that targeted the *ntla* (Figure S2), and *oep* (Figure S3) genes were selected.

Transient in vivo RNAi is highly potent in knocking down gene activity

For functional validation of shRNAs, we employed a transient *in vivo* transgenesis method. Although the mosaic expression is an inevitable feature associated with transient transgenesis, this can be alleviated by coexpression of the Tol2 transposase (Li *et al.* 2010) and selection of high

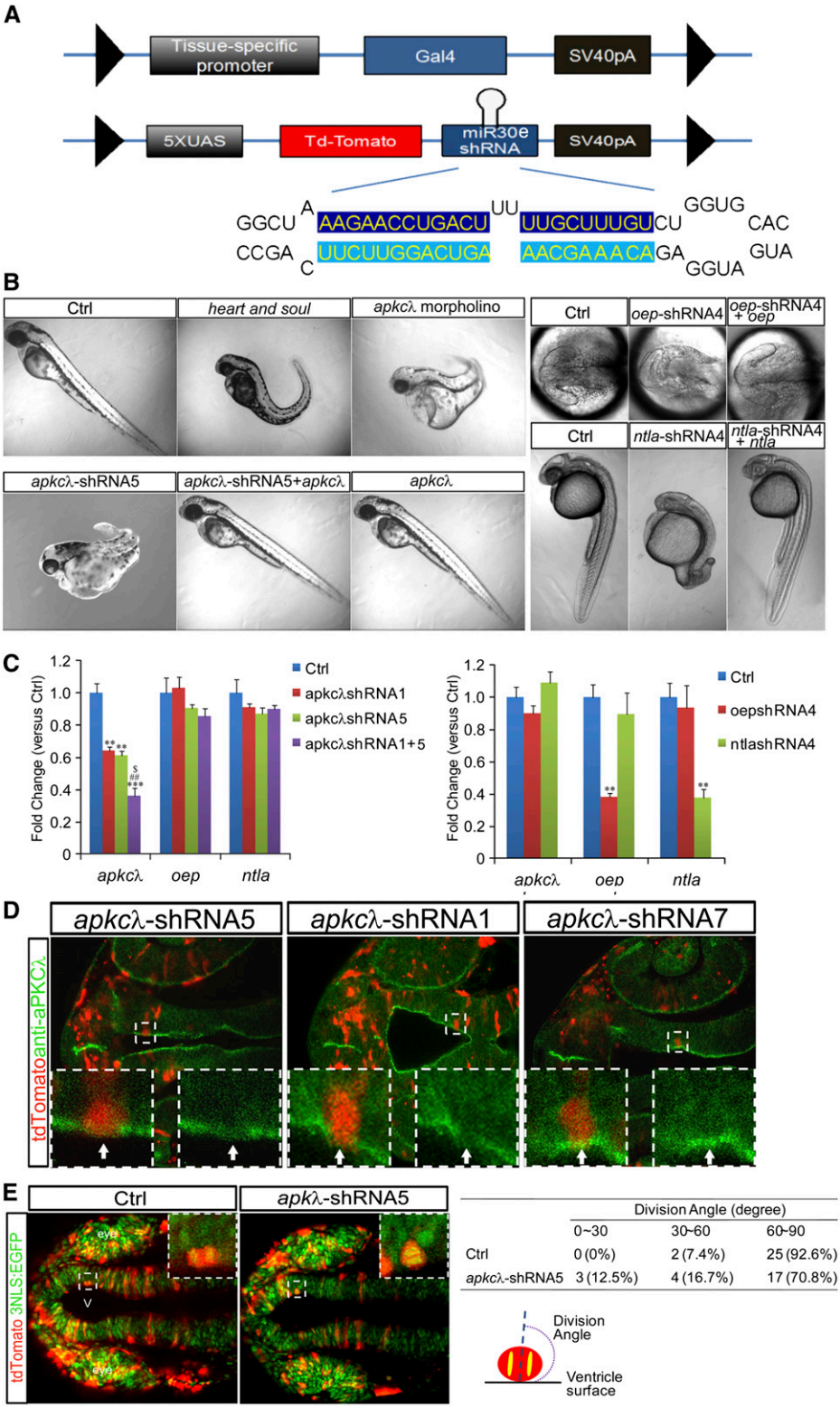

Figure 1 Functional validation of miR-shRNAs by transient *in vivo* transgenesis. (A) Diagram of the conditional miR-shRNA expression system. The guide stand (bottom) is highlighted in light blue. (B) Mosaic expression of miR-shRNA5$^{apkc\lambda}$ (left), miR-shRNA4^{oep} (top right), and miR-shRNA4^{ntla} (bottom right) causes morphological defects similar to those observed in respective mutants, which can be rescued by delivery of shRNA-resistant wild-type mRNAs. The miR-30e vector-injected embryos serve as controls. (C) Quantitative RT–PCR analysis shows a gene-specific reduction of endogenous mRNA levels by shRNAs cognate to their target genes. The miR-30e vector-injected embryos serve as controls. (D) Fluorescent immunostaining of aPKCλ (green) shows knockdown effects at the protein level by different miR-shRNAs$^{apkc\lambda}$. In a single miR-shRNA$^{apkc\lambda}$-expressing cell, as indicated by the tdTomato fluorescence (red), miR-shRNA1$^{apkc\lambda}$ (middle panel) and miR-shRNA5$^{apkc\lambda}$ (left panel) lead to significant knockdown of aPKCλ, whereas the ineffective miR-shRNA7$^{apkc\lambda}$ does not show obvious knockdown effect (right panel). (E) Mosaic expression of miR-shRNA5$^{apkc\lambda}$ causes defects in mitotic division orientation of radial glia progenitors in the developing zebrafish forebrain. Left: examples of mitotic division orientation in the miR-30e vector-injected (control) and miR-shRNA5$^{apkc\lambda}$-expressing radial glia progenitors. Right: Quantification of division orientation in miR-30e vector control and miR-shRNA5$^{apkc\lambda}$-expressing radial glia progenitors (n = 27 for control, and n = 24 for miR-shRNA5$^{apkc\lambda}$). The nuclei of radial glia progenitors were labeled with 3NLS:EGFP (green) and the individual radial glia progenitors expressing *UAS-miR30e* vector (control) or *UAS-miR-shRNA5*$^{apkc\lambda}$ were highlighted by tdTomato (red).

expressers with the visible reporter TdTomato (Figure S4). DNA plasmids carrying the *Pef-1a-Gal4* (elongation factor 1a promoter-driven Gal4) and *UAS-miR-shRNA* together with the transposase were co-injected into one-cell-stage zebrafish embryos. Three of six *miR-shRNAs* targeting *apkcλ*, and three of four *miR-shRNAs* targeting either *oep* or *ntla* genes led to gene-specific phenotypes (with variable penetrance) that could be rescued by delivery of shRNA-resistant wild-type mRNAs for the respective genes (Figure 1B, Table S1, Table S2, and Table S3). Quantitative RT–PCR analysis using total RNAs from 10 hpf shRNA-expressing embryos showed a gene-specific reduction of endogenous mRNAs

cognate to the shRNA target genes, and codelivery of two shRNAs (1 + 5) targeting *apkcλ* further decreased the endogenous *apkcλ* level (Figure 1C). Immunostaining of the aPKC protein (recognizing both λ and θ isoforms) showed at single-cell levels that the two most effective shRNAs, *apkcλ-shRNA5* and *apkcλ-shRNA1*, diminished the apically localized aPKC protein in radial glia progenitors, whereas the ineffective apkcλ-shRNA7 did not (Figure 1D).

Transient in vivo RNAi is a powerful tool for genetic mosaic analysis

A useful application of transient RNAi is *in vivo* genetic mosaic analysis at single-cell resolution. Using time-lapse imaging, we further analyzed the miR-shRNA-expressing individual radial glia progenitor cells for the mitotic spindle rotation phenotype associated with the loss of *apkcλ* gene activity (Horne-Badovinac *et al.* 2001). While most control progenitors (>90%) displayed a division angle between 60° and 90° and none between 0° and 30° (Figure 1E and File S1), a significant portion of the *apkcλ-shRNA5*-expressing progenitors had a division angle between either 0° and 30° or 30° and 60° (Figure 1E and File S2), a ratio that was similar to what has been observed in the *apkcλ* mutant (*heart and soul, has*) retina (Horne-Badovinac *et al.* 2001). Together, these results validate the efficacy and specificity of miR-shRNAs *in vivo* and demonstrate the saliency of transient RNAi for *in vivo* genetic mosaic analysis at single-cell resolution.

Stable gene silencing with UAS-miR-shRNA^{apkcλ} transgenic lines

Next we established transgenic lines that carry the *UAS-TdTom-miR-shRNA1^{apkcλ}* or *UAS-TdTom-miR-shRNA5^{apkcλ}* transgene using the Tol2 transposon system. G_0 germ-line transgenic founders were identified as those that produced red fluorescent progeny when crossed with the *Ubiquitous-Gal4* (*Ubi-GFF*) transgenic animal (Asakawa and Kawakami 2010). One of 40 *UAS-TdTom-miR-shRNA1^{apkcλ}* and 3 of 50 *UAS-TdTom-miR-shRNA5^{apkcλ}* founders transmitted the transgenes to germ line (Figure 2A, Table S4, and Table S5). We noted that among the F_1's derived from the *UAS-TdTom-miR-shRNA1^{apkcλ}* founder (A) and Tg[*Ubi-GFF*] cross, ~30% of the TdTom-positive embryos displayed a heart defect with cardiac edema that was strictly correlated with the expression of TdTom (Figure 2B, middle panels compared to top panels). This heart defect was rescued by the delivery of shRNA-resistant *apkcλ* mRNA (Figure 2, B, bottom panels, and C). Furthermore, to test for the spatiotemporal effect of RNAi, we crossed the *UAS-TdTom-miR-shRNA1^{apkcλ}* founder (A) with Tg [*hsp-gal4*], and subjected the resulting embryos to a transient heat shock. The data showed an shRNA-dependent cardiac defect upon heat shock (Figure 2D). Together, these results demonstrate the stable integration and germ-line transmission of RNAi in zebrafish and uncover a cardiac impairment by *UAS-TdTom-miR-shRNA1^{apkcλ}* that is temporally regulatable.

To determine whether a greater impairment of *apkcλ* gene activity might be achievable if the strength of the Gal4 driver was increased, we used KalTA4, an optimized version of Gal4 for zebrafish (Distel *et al.* 2009). The KalTA4 mRNA was injected into one-cell stage-F_2 embryos from *Tg [UAS-TdTom-miR-shRNA1^{apkcλ} A*; *Ubi-GFF]* fish. While the KalTA4 mRNA-injected, nontransgenic siblings were mostly normal, KalTA4 mRNA-injected, TdTom-positive transgenic embryos showed an *apkcλ* mutant-like morphology (Figure 2E, 4 and Table S6). Similarly, *EF1α-GFF* DNA-injected, TdTom-positive transgenic embryos also showed an *apkcλ* mutant-like phenotype (Figure 2E, 5 and Table S7). To assess the endogenous *apkcλ* mRNA level, we employed the Droplet Digital (dd) PCR technology (Figure S5), which measures target (*e.g.*, *apkcλ* mRNA) and control (*e.g.*, *gapdh* mRNA) molecules in the same biological reaction for superb precision and sensitivity (Hua *et al.* 2010). The results showed a clear correlation between the phenotypic severity and the *apkcλ* mRNA knockdown level (Figure 2E). Together, these results uncover a dosage-dependent knockdown of *apkcλ* gene activity through stable *UAS-miR-shRNA* transgenesis and controllable expression of Gal4.

Conclusions

We show that RNAi employing the miR-shRNA and Gal4/UAS system is a promising technology for conditional gene silencing in zebrafish. Compared to previous reports (Dong *et al.* 2009; De Rienzo *et al.* 2012), our bipartite Gal4/UAS-based design offers greater versatility and synergizes with the ongoing development of Gal4 enhancer trap lines in zebrafish.

Two platforms are established that can be used either independently or in combination to serve different research needs. The first platform is the *in vivo* transient RNAi. We demonstrate that this method leads to robust and specific phenotypes associated with three different genes, *apkcλ*, *oep*, and *ntla*. We also show that it is a powerful tool for genetic mosaic analysis at single-cell resolution. The ability to detect significant and dosage-dependent decrease of target mRNA expression also makes the *in vivo* transient RNAi a high throughput screening tool for identifying effective miR-shRNAs. The second platform is the *in vivo* stable RNAi. We show that the miR-shRNA transgenes can be stably inherited in subsequent generations and leads to significant gene knockdown that is temporally regulatable and dependent on the strength and expression of the Gal4 driver.

However, it is worth pointing out that the stable *UAS-shRNA^{apkcλ}* transgene, which is likely present at single or few copies in the genome, is insufficient to produce the severe mutant phenotype observable in transient RNAi, when crossed with stable Gal4 lines including several tissue-specific Gal4 lines tested. This is likely to be a general concern associated with stable RNAi, and is possibly due to the difference in shRNA transgene copy numbers between transient and stable RNAi. Increasing the *UAS-shRNA* copy

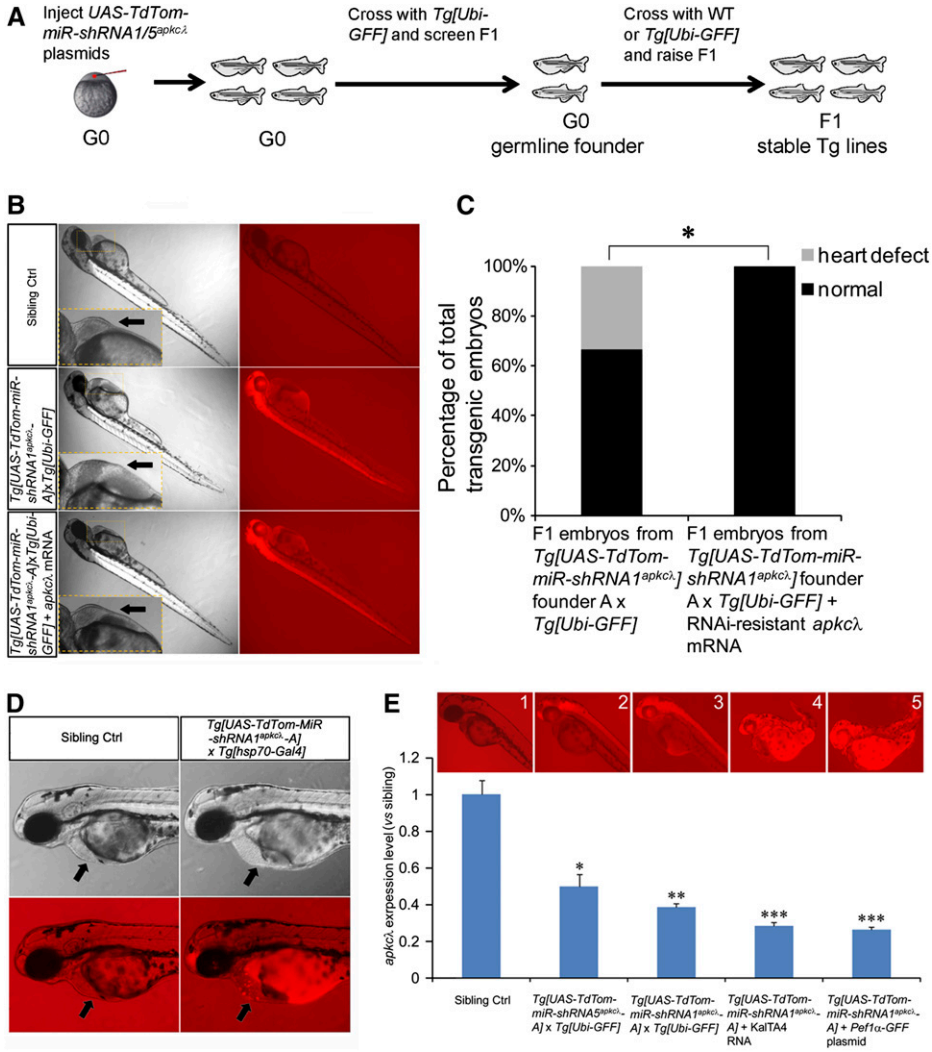

Figure 2 Functional validation of miR-shRNAs by stable *in vivo* transgenesis. (A) Schematic shows the stable transgenesis of miR-shRNAs$^{apkc\lambda}$ in zebrafish using the Tol2 transposon system. (B) F_1 embryos derived from a cross between the *UAS-TdTom-miR-shRNA1*$^{apkc\lambda}$ founder A and *Ubi-GFF* transgenic line. TdTom-negative F_1 embryos are normal (top panels). In contrast, ~30% of the TdTom-positive F_1 embryos display a heart defect with cardiac edema (middle panels). This heart defect is rescued by the delivery of shRNA-resistant *apkcλ* mRNA (bottom panels). (C) Quantification of heart defect and rescue in B. (D) Embryos (60 hpf) derived from a cross between the *UAS-TdTom-miR-shRNA1*$^{apkc\lambda}$ founder A and *hsp70-Gal4* transgenic animal. Heat shock was performed at 8 hpf at 37 °C for 1 hr. The TdTom-positive embryo (right) displayed a heart defect with cardiac edema, whereas the heat-shocked control sibling (left) did not. (E) Droplet digital PCR analyses of endogenous *apkcλ* mRNA levels in stable *UAS-TdTom-miR-shRNAs*$^{apkc\lambda}$ transgenic lines at different conditions of Gal4 induction. The representative images of 48-hpf embryos for each condition were shown on top of the bar graph. $*P < 0.05$, $**P < 0.01$, $***P < 0.001$, *vs.* control sibling.

numbers through homozygosing the transgene or crossing two different *UAS-shRNA* lines that potentially quadruples the copy numbers did not produce an obvious difference in our hands, suggesting a great many more copy numbers are necessary to produce a transient RNAi-like effect in stable lines. It may not be feasible to incorporate tens or hundreds of miR-shRNA copies in the transgene for concerns of cloning and transgene stability. Instead, the efficacy of stable RNAi transgenic systems may be further enhanced by incorporating the dual Tet-regulatory system (Knopf *et al.* 2010) recently developed in zebrafish for further amplifying the UAS transgene expressivity. Taken together, this study demonstrates the first prototype of stable and conditional RNAi-mediated gene silencing employing the Gal4/UAS system in zebrafish that has the potential to transform the utility of this vertebrate for uncovering novel biology and modeling human diseases.

Acknowledgments

We thank the late Tingxi Liu for the zebrafish miR-30e vector; Kazuhide Asakawa and Koichi Kawakami for the Ubi-GFF transgenic line; the Guo lab and B. Lu for helpful discussions and comments on the manuscript; Camille Troup and David Merrium from the Bio-Rad Laboratories for discussion on the dd-PCR technology; and David Merrium for generously providing access to the equipment and for technical advice. This work was supported by National Institutes of Health grants (NS042626 and DA023904).

Literature Cited

Aitman, T. J., C. Boone, G. A. Churchill, M. O. Hengartner, T. F. Mackay *et al.*, 2011 The future of model organisms in human disease research. Nat. Rev. Genet. 12: 575–582.

Asakawa, K., and K. Kawakami, 2010 A transgenic zebrafish for monitoring in vivo microtubule structures. Dev. Dyn. 239: 2695–2699.

Bartel, D. P., 2009 MicroRNAs: target recognition and regulatory functions. Cell 136: 215–233.

Bedell, V. M., Y. Wang, J. M. Campbell, T. L. Poshusta, C. G. Starker *et al.*, 2012 In vivo genome editing using a high-efficiency TALEN system. Nature **491:** 114–118.

Davis, R. H., 2004 The age of model organisms. Nat. Rev. Genet. 5: 69–76.

De Rienzo, G., J. H. Gutzman, and H. Sive, 2012 Efficient shRNA-mediated inhibition of gene expression in zebrafish. Zebrafish 9: 97–107.

Dickins, R. A., M. T. Hemann, J. T. Zilfou, D. R. Simpson, I. Ibarra *et al.*, 2005 Probing tumor phenotypes using stable and regulated synthetic microRNA precursors. Nat. Genet. 37: 1289–1295.

Distel, M., M. F. Wullimann, and R. W. Köster, 2009 Optimized Gal4 genetics for permanent gene expression mapping in zebrafish. Proc. Natl. Acad. Sci. USA 106: 13365–13370.

Dong, M., Y. F. Fu, T. T. Du, C. B. Jing, C. T. Fu *et al.*, 2009 Heritable and lineage-specific gene knockdown in zebrafish embryo. PLoS ONE 4: e6125.

Dong, Z., N. Yang, S. Yeo, A. Chitnis, and S. Guo, 2012 Intralineage directional Notch signaling regulates self-renewal and differentiation of asymmetrically dividing radial glia. Neuron 74: 65–78.

Doyon, Y., J. M. McCammon, J. C. Miller, F. Faraji, C. Ngo *et al.*, 2008 Heritable targeted gene disruption in zebrafish using designed zinc-finger nucleases. Nat. Biotechnol. 26: 702–708.

Ebert, M. S., and P. A. Sharp, 2012 Roles for microRNAs in conferring robustness to biological processes. Cell 149: 515–524.

Elbashir, S. M., J. Harborth, W. Lendeckel, A. Yalcin, K. Weber *et al.*, 2001 Duplexes of 21-nucleotide RNAs mediate RNA interference in cultured mammalian cells. Nature 411: 494–498.

Fire, A., S. Xu, M. K. Montgomery, S. A. Kostas, S. E. Driver *et al.*, 1998 Potent and specific genetic interference by double-stranded RNA in Caenorhabditis elegans. Nature 391: 806–811.

Fire, A. Z., 2007 Gene silencing by double-stranded RNA. Cell Death Differ. 14: 1998–2012.

Gruber, J., H. Manninga, T. Tuschl, M. Osborn, and K. Weber, 2005 Specific RNAi mediated gene knockdown in zebrafish cell lines. RNA Biol. 2: 101–105.

Guo, S., and K. J. Kemphues, 1995 par-1, a gene required for establishing polarity in C. elegans embryos, encodes a putative ser/thr kinase that is asymmetrically distributed. Cell 81: 611–620.

Guo, S., S. W. Wilson, S. Cooke, A. B. Chitnis, W. Driever *et al.*, 1999 Mutations in the zebrafish unmask shared regulatory pathways controlling the development of catecholaminergic neurons. Dev. Biol. 208: 473–487.

Horne-Badovinac, S., D. Lin, S. Waldron, M. Schwarz, G. Mbamalu *et al.*, 2001 Positional cloning of heart and soul reveals multiple roles for PKC lambda in zebrafish organogenesis. Curr. Biol. 11: 1492–1502.

Hua, Z., J. L. Rouse, A. E. Eckhardt, V. Srinivasan, V. K. Pamula *et al.*, 2010 Multiplexed real-time polymerase chain reaction on a digital microfluidic platform. Anal. Chem. 82: 2310–2316.

Huang, P., A. Xiao, M. Zhou, Z. Zhu, S. Lin *et al.*, 2011 Heritable gene targeting in zebrafish using customized TALENs. Nat. Biotechnol. 29: 699–700.

Knopf, F., K. Schnabel, C. Haase, K. Pfeifer, K. Anastassiadis *et al.*, 2010 Dually inducible TetON systems for tissue-specific conditional gene expression in zebrafish. Proc. Natl. Acad. Sci. USA 107: 19933–19938.

Lee, R. C., R. L. Feinbaum, and V. Ambros, 1993 The C. elegans heterochronic gene lin-4 encodes small RNAs with antisense complementarity to lin-14. Cell 75: 843–854.

Li, Q., D. Ritter, N. Yang, Z. Dong, H. Li *et al.*, 2010 A systematic approach to identify functional motifs within vertebrate developmental enhancers. Dev. Biol. 337: 484–495.

Manche, L., S. R. Green, C. Schmedt, and M. B. Mathews, 1992 Interactions between double-stranded RNA regulators and the protein kinase DAI. Mol. Cell. Biol. 12: 5238–5248.

Mello, C. C., 2007 Return to the RNAi world: rethinking gene expression and evolution. Cell Death Differ. 14: 2013–2020.

Meng, X., M. B. Noyes, L. J. Zhu, N. D. Lawson, and S. A. Wolfe, 2008 Targeted gene inactivation in zebrafish using engineered zinc-finger nucleases. Nat. Biotechnol. 26: 695–701.

Nasevicius, A., and S. C. Ekker, 2000 Effective targeted gene "knockdown" in zebrafish. Nat. Genet. 26: 216–220.

Paddison, P. J., A. A. Caudy, E. Bernstein, G. J. Hannon, and D. S. Conklin, 2002 Short hairpin RNAs (shRNAs) induce sequence-specific silencing in mammalian cells. Genes Dev. 16: 948–958.

Premsrirut, P. K., L. E. Dow, S. Y. Kim, M. Camiolo, C. D. Malone *et al.*, 2011 A rapid and scalable system for studying gene function in mice using conditional RNA interference. Cell 145: 145–158.

Ptashne, M., 1988 How eukaryotic transcriptional activators work. Nature 335: 683–689.

Reinhart, B. J., F. J. Slack, M. Basson, A. E. Pasquinelli, J. C. Bettinger *et al.*, 2000 The 21-nucleotide let-7 RNA regulates developmental timing in Caenorhabditis elegans. Nature 403: 901–906.

Sander, J. D., L. Cade, C. Khayter, D. Reyon, R. T. Peterson *et al.*, 2011 Targeted gene disruption in somatic zebrafish cells using engineered TALENs. Nat. Biotechnol. 29: 697–698.

Schulte-Merker, S., F. J. van Eeden, M. E. Halpern, C. B. Kimmel, and C. Nüsslein-Volhard, 1994 no tail (ntl) is the zebrafish homologue of the mouse T (Brachyury) gene. Development 120: 1009–1015.

Silva, J. M., M. Z. Li, K. Chang, W. Ge, M. C. Golding *et al.*, 2005 Second-generation shRNA libraries covering the mouse and human genomes. Nat. Genet. 37: 1281–1288.

Stark, G. R., I. M. Kerr, B. R. Williams, R. H. Silverman, and R. D. Schreiber, 1998 How cells respond to interferons. Annu. Rev. Biochem. 67: 227–264.

Suster, M. L., H. Kikuta, A. Urasaki, K. Asakawa, and K. Kawakami, 2009 Transgenesis in zebrafish with the tol2 transposon system. Methods Mol. Biol. 561: 41–63.

Ui-Tei, K., Y. Naito, K. Nishi, A. Juni, and K. Saigo, 2008 Thermodynamic stability and Watson-Crick base pairing in the seed duplex are major determinants of the efficiency of the siRNA-based off-target effect. Nucleic Acids Res. 36: 7100–7109.

Wang, L., J. Y. Zhou, J. H. Yao, D. R. Lu, X. J. Qiao *et al.*, 2010 U6 promoter-driven siRNA injection has nonspecific effects in zebrafish. Biochem. Biophys. Res. Commun. 39: 1363–1368.

Wienholds, E., S. Schulte-Merker, B. Walderich, and R. H. A. Plasterk, 2002 Target-selected inactivation of the zebrafish rag1 gene. Science 297: 99–102.

Zeng, Y., E. J. Wagner, and B. R. Cullen, 2002 Both natural and designed micro RNAs can inhibit the expression of cognate mRNAs when expressed in human cells. Mol. Cell 9: 1327–1333.

Zhang, J., W. S. Talbot, and A. F. Schier, 1998 Positional cloning identifies zebrafish one-eyed pinhead as a permissive EGF-related ligand required during gastrulation. Cell 92: 241–251.

Zhao, X. F., A. Fjose, N. Larsen, J. V. Helvik, and Ø. Drivenes, 2008 Treatment with small interfering RNA affects the microRNA pathway and causes unspecific defects in zebrafish embryos. FEBS J. 275: 2177–2184.

Zuber, J., K. McJunkin, C. Fellmann, L. E. Dow, M. J. Taylor *et al.*, 2011 Toolkit for evaluating genes required for proliferation and survival using tetracycline-regulated RNAi. Nat. Biotechnol. 29: 79–83.

Communicating editor: B. Goldstein

GENETICS

Supporting Information
http://www.genetics.org/lookup/suppl/doi:10.1534/genetics.112.147892/-/DC1

Stable Gene Silencing in Zebrafish with Spatiotemporally Targetable RNA Interference

Zhiqiang Dong, Jisong Peng, and Su Guo

DOI: 10.1534/genetics.112.147892

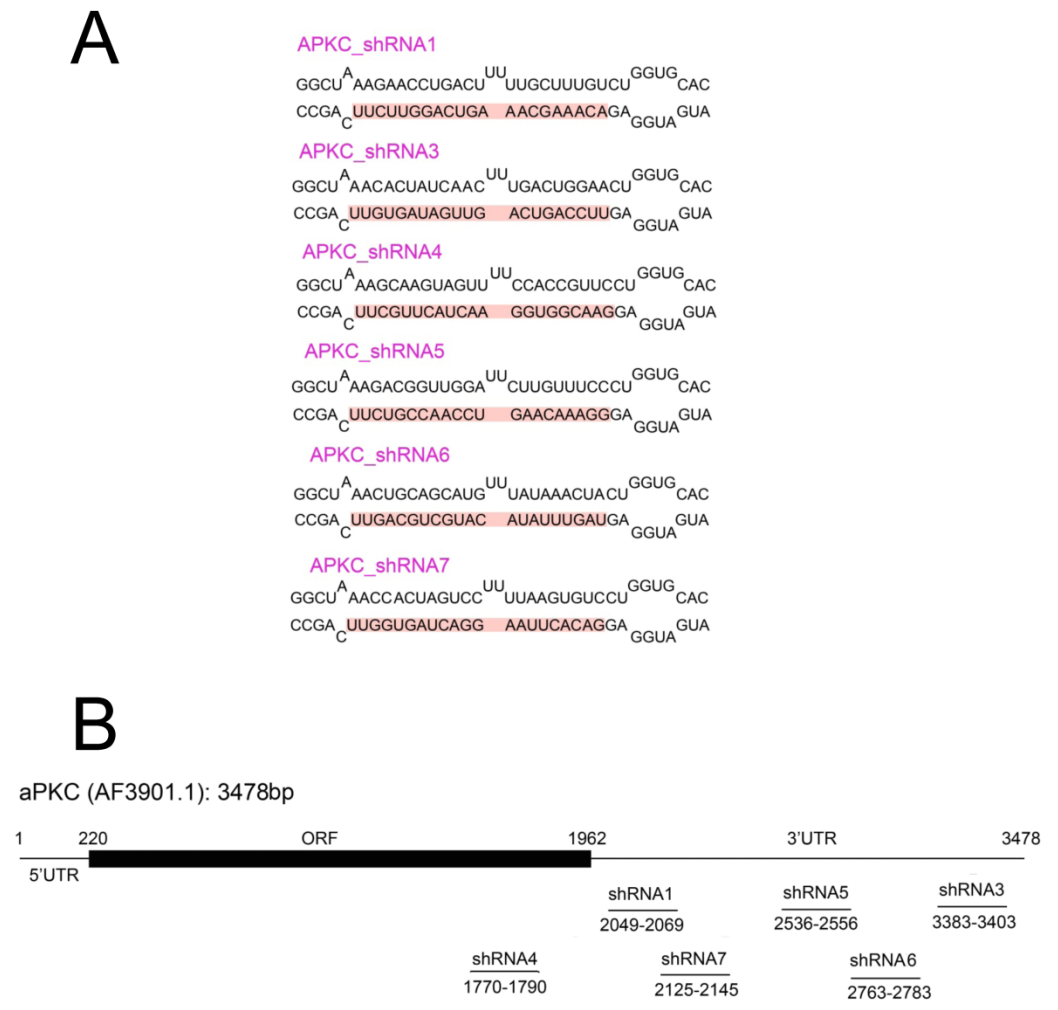

Figure S1 The design of miR-shRNAs targeting *apkcλ*. (A) The sequences of six shRNAs targeting *apkcλ*. The guide strands are highlighted in pink. (B) The location of shRNA target sites in the *apkcλ* mRNA.

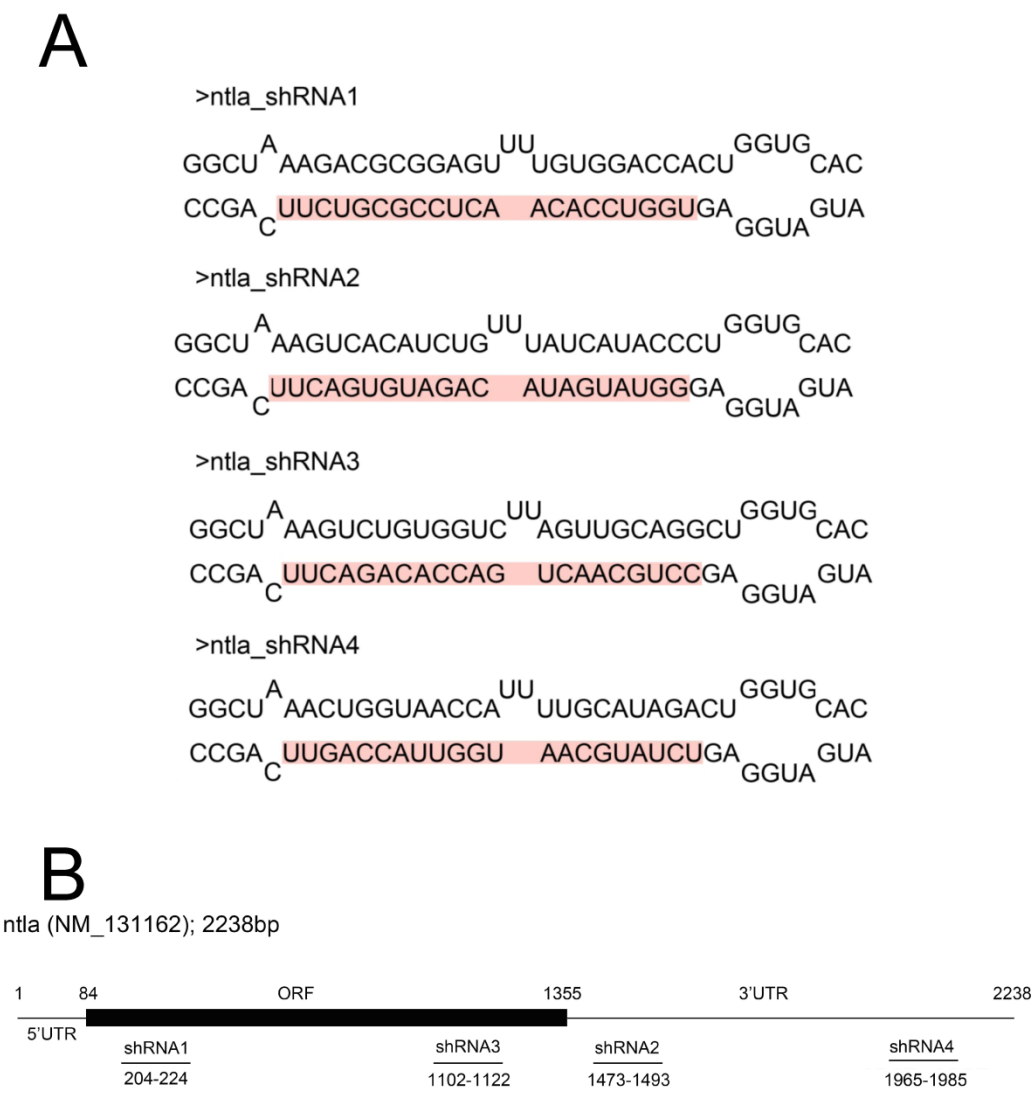

Figure S2 The design of miR-shRNAs targeting *ntla*. (A) The sequences of four shRNAs targeting *ntla*. The guide strands are highlighted in pink. (B) The location of shRNA target sites in the *ntla* mRNA.

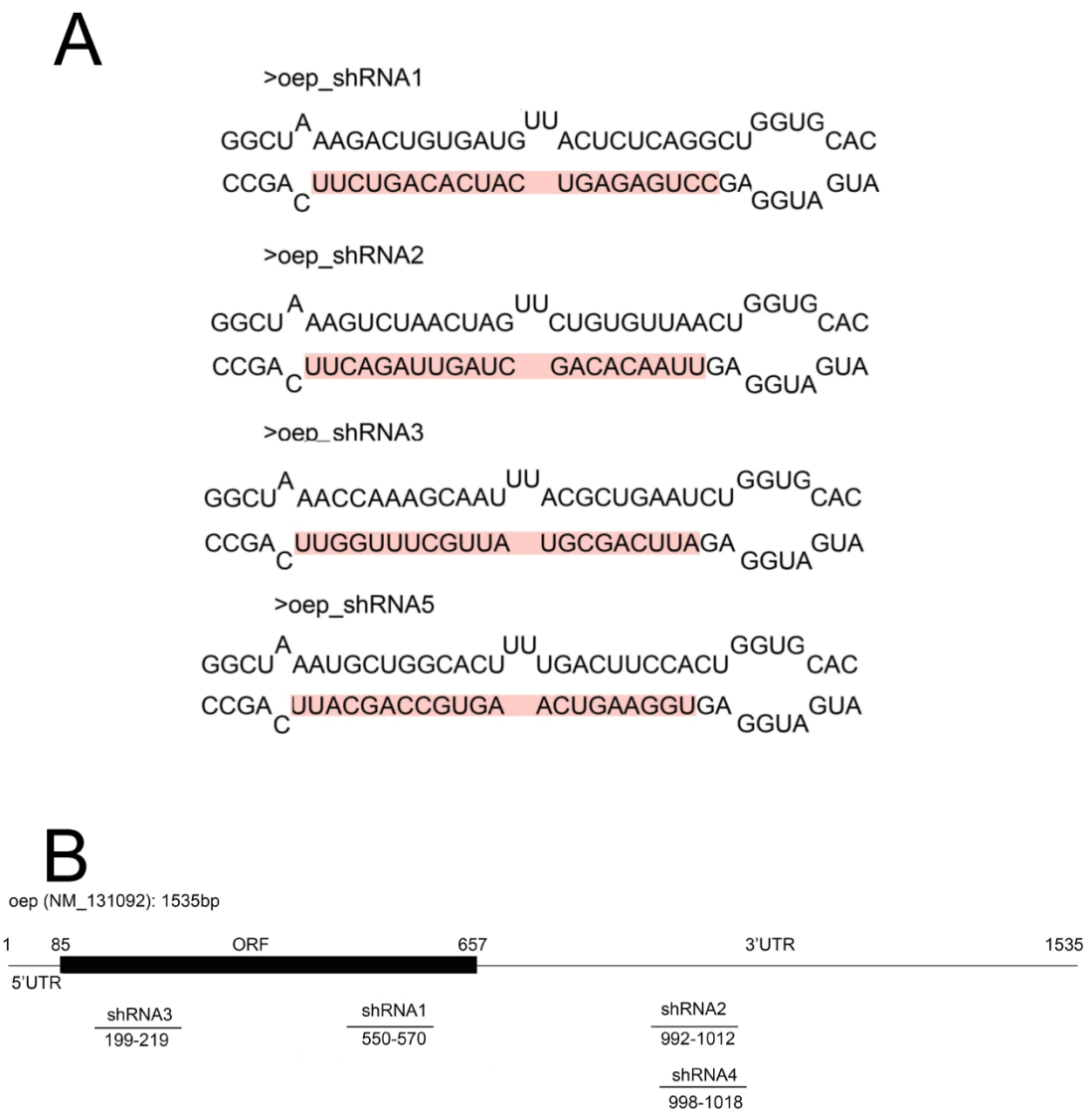

Figure S3 The design of miR-shRNAs targeting *oep*. (A) The sequences of four shRNAs targeting *oep*. The guide strands are highlighted in pink. (B) The location of shRNA target sites in the *oep* mRNA.

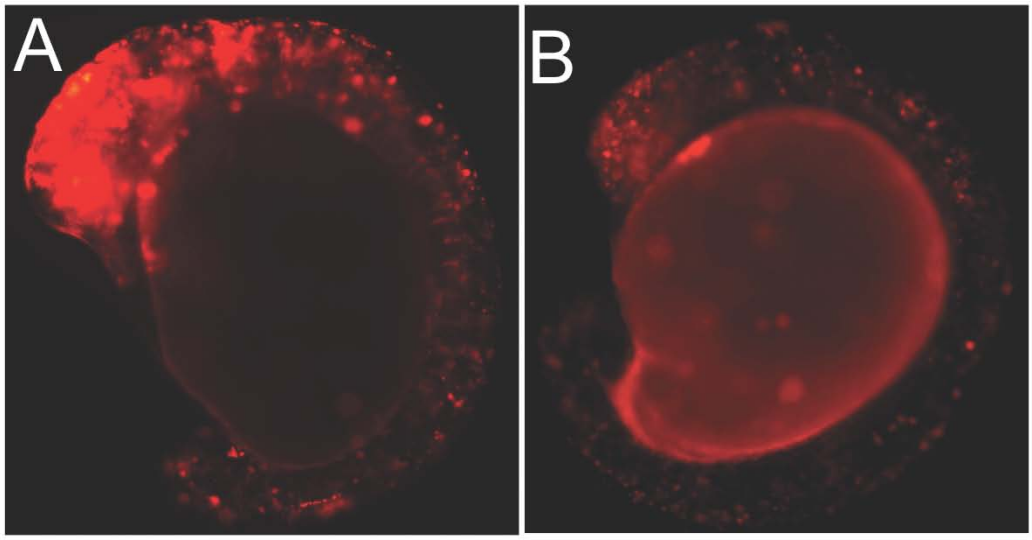

Figure S4 Representative images of TdTom-miR-shRNA expressing embryos in transient transgenesis. (A) The embryo with low expression mosaicism, which is used for our analysis. (B) The embryo with high expression mosaicism, which is not used for our analysis.

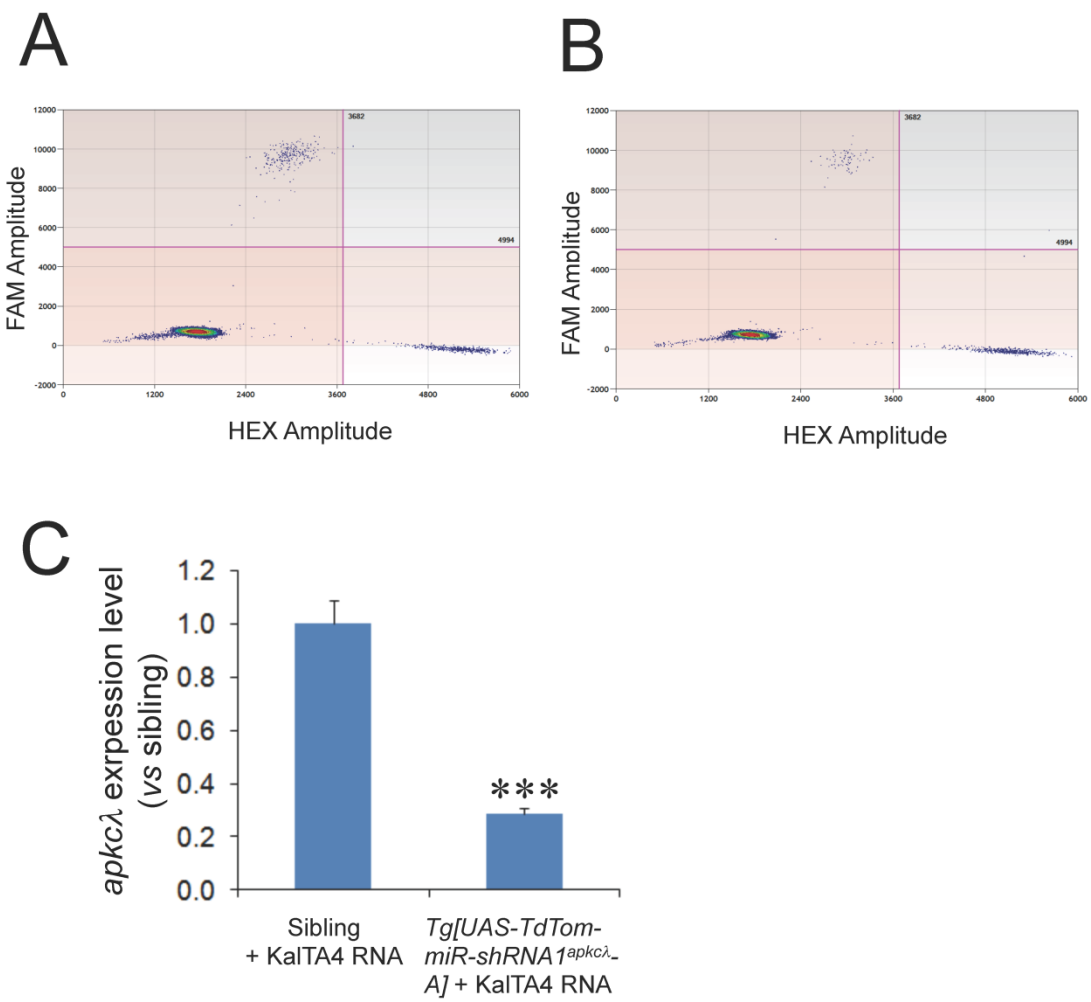

Figure S5 Droplet Digital PCR analyses of endogenous *apkcλ* mRNA levels in stable *UAS-TdTom-miR-shRNA*$^{apkc\lambda}$ transgenic lines coupled with the KalTA4 driver. (A-B) FAM intensity plotted against HEX intensity. (A) Sibling control embryos injected with KalTA4 RNA. (B) *UAS-TdTom-miR-shRNA1*$^{apkc\lambda}$*-A* transgenic embryos injected with KalTA4 RNA. In both (A) and (B), pink lines are thresholds used to assign individual droplets as either positive or negative, which divide the graph into four sections: top left (droplets positive for *apkcλ*), top right (droplets positive for both *apkcλ* and *gapdhs*), bottom right (droplets positive for *gapdhs*) and bottom left (negative droplets with quenched un-hydrolyzed probes). With similar amount of *gapdhs* positive droplets, (b) shows less *apkcλ* positive droplets compared with (A), indicating reduced *apkcλ* mRNA level. (C) Statistic analysis on Droplet Digital PCR results of (A) and (B). *: $P < 0.05$, **: $P < 0.01$, *vs* sibling.

File S1

Time-lapse of a single *TdTom-miR-30e* vector control -expressing radial glia progenitor during mitotic division. The division ends at an angle close to 90 degree. The interval between each frame is 90 seconds.

File S1 is available for download at http://www.genetics.org/lookup/suppl/doi:10.1534/genetics.112.147892/-/DC1.

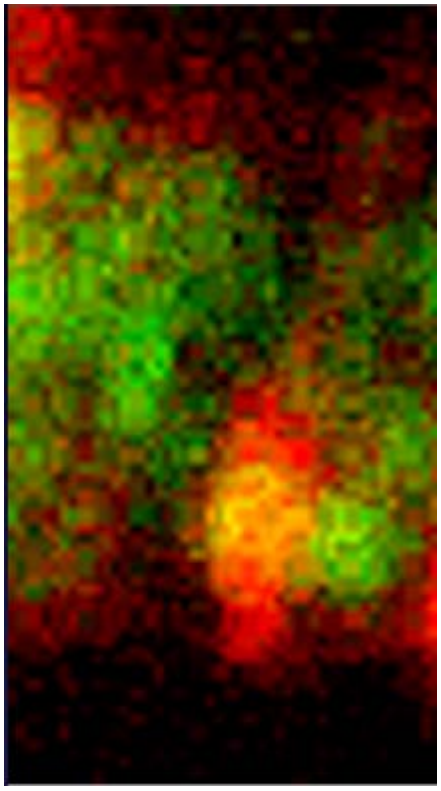

screenshot from File S1

File S2

Time-lapse of a single *TdTom-miR-shRNA5*$^{apkc\lambda}$ -expressing radial glia progenitor during mitotic division. The mitotic spindle undergoes active rotation and the division ends at an angle close to 0 degree. The interval between each frame is 90 seconds.

File S2 is available for download at http://www.genetics.org/lookup/suppl/doi:10.1534/genetics.112.147892/-/DC1.

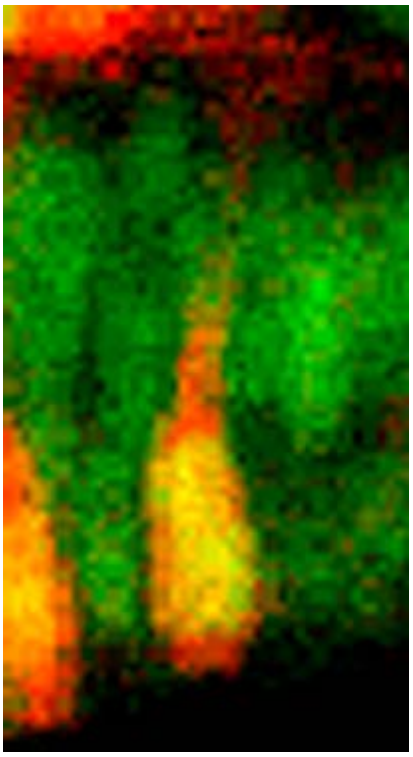

screenshot from File S2

Table S1 The efficacy and specificity of different *apkcλ*-shRNAs based on morphological phenotypes. *UAS-TdTom-miR-shRNA$^{apkc\lambda}$-miniTol2* plasmid was co-injected with *Pef1α-GFF-PT2KXIG* and Tol2 transposase into wild-type embryos at 1-cell stage and phenotypes were analyzed at ~48 hpf. The shRNA-resistant *apkcλ* mRNA (coding region only) was used for rescue. The miR-30e vector –injected embryos served as controls. *: $P < 0.05$; **: $P < 0.01$; ***: $P < 0.001$ vs Ctrl., ##: $P < 0.01$; ###: $P < 0.001$ *vs apkcλ*-shRNA5, Z-test.

	Embryos with broad and strong tdTomato expression	Embryos with defective heart tube	Embryos with abnormal body curvature	Embryos with patchy RPE	Embryos with abnormally narrow brain ventricle
Ctrl.	46	2 (4.35%)	2 (4.35%)	0 (0.00%)	1 (2.17%)
apkcλ–shRNA1	39	12 (30.77%)**	9 (23.08%)*	10 (25.64%)***	7 (17.95%)*
apkcλ–shRNA3	32	9 (28.13%)**	7 (21.88%)*	5 (15.63%)*	5(15.63%)
apkcλ–shRNA4	34	6 (17.65%)	5 (14.71%)	4 (11.76%)	4 (11.76%)
apkcλ–shRNA5	50	21 (42.00%)***	17 (34.00%)***	19 (38.00%)***	14 (28.00%)**
apkcλ–shRNA5+ *apkcλ* RNA	56	8 (14.29%)##	6 (10.71%)##	2 (3.57%)###	4 (7.14%)##
apkcλ–shRNA6	36	6 (16.67%)	4 (11.11%)	3 (8.33%)	3 (8.33%)
apkcλ–shRNA7	37	5 (13.51%)	3 (8.11%)	4 (10.81%)	3 (8.11%)

Table S2 The efficacy and specificity of different *ntla*-shRNAs based on morphological phenotypes. miR-*ntla*-shRNA (in pCS2) was *in vitro* transcribed and injected into wild-type embryos at 1-cell stage and phenotypes were analyzed at ~24 hpf. The shRNA-resistant *ntla* mRNA (coding region only) was used for rescue. The miR-30e vector –injected embryos served as controls. **: $P < 0.01$; ***: $P < 0.001$ vs Ctrl., ###: $P < 0.001$ *vs ntla*-shRNA4, Z-test.

	Embryos injected with ctrl RNA or *ntl*- shRNAs	Embryos with no tail phenotype
Ctrl.	53	0 (0.00%)
ntla-shRNA1	56	9 (16.07%)**
ntla-shRNA2	52	10(19.23%)**
ntla-shRNA3	61	5 (8.20%)
ntla-shRNA4	49	23 (46.94%)***
ntla-shRNA4 + *ntla* RNA	57	4 (7.02%)###

Table S3 The efficacy and specificity of different *oep*-shRNAs based on morphological phenotypes. miR-*oep*-shRNA RNA (in pCS2) was in vitro transcribed and injected into wild-type embryos at 1-cell stage and phenotypes were analyzed at ~24 hpf. The shRNA-resistant *oep* mRNA (coding region only) was used for rescue. The miR-30e vector –injected embryos served as controls. **: $P < 0.01$; ***: $P < 0.001$ vs Ctrl., ##: $P < 0.01$ *vs oep*-shRNA4, Z-test.

	Embryos injected with ctrl RNA or *oep*-shRNAs	Embryos with one-eyed and pinhead phenotype
Ctrl.	51	0 (0.00%)
oep-shRNA1	49	0 (0.00%)
oep-shRNA2	42	9 (21.43%)**
oep-shRNA3	50	10 (20.00%)**
oep-shRNA4	52	16 (30.77%)***
oep-shRNA4 + *oep* RNA	56	3 (5.36%)##

Table S4 Summary of stable transgenic lines carrying either *UAS-TdTom-miR-shRNA1$^{apkc\lambda}$* or *UAS-TdTom-miR-shRNA5$^{apkc\lambda}$*.

Transgenic constructs	# G0 founder fish x *Tg [Ubi-GFF]*	# G0 germ-line transgenic founders identified	% F1 that are transgenic (TdTomato positive)	% transgenic F1s with rescuable knockdown phenotype
UAS-miR-shRNA1$^{apkc\lambda}$	40	1 (Founder A)	~3%	30%
UAS-miR-shRNA5$^{apkc\lambda}$	50	3 (Founder A, B, C)	~5%	N.A.

Table S5 Summary of morphological phenotypes of *UAS-TdTom-miR-shRNA1$^{apkc\lambda}$* or *UAS-TdTom-miR-shRNA5$^{apkc\lambda}$* transgenic lines when crossed with *Ubi-GFF* transgenic line.

# Tg lines	UAS-miR-shRNA1$^{apkc\lambda}$ A	UAS-miR-shRNA5$^{apkc\lambda}$ A	UAS-miR-shRNA5$^{apkc\lambda}$ B	UAS-miR-shRNA5$^{apkc\lambda}$ C
Phenotype x *Tg [Ubi-GFF]*	cardiac defect	normal	normal	normal

Table S6 Summary of morphological phenotypes of *UAS-TdTom-miR-shRNA1$^{apkc\lambda}$*-A transgenic lines injected with KalTA4 RNA. ***: *P*< 0.001, vs Sibling + KalTA4 RNA.

	Number of embryos	Embryos with defective heart tube	Embryos with abnormal body curvature	Embryos with patchy RPE	Embryos with abnormally narrow brain ventricle
Sibling + KalTA4 RNA	46	3 (6.52%)	2 (4.35%)	0 (0.00%)	2 (4.35%)
Tg[UAS-TdTom-miR-shRNA1$^{apkc\lambda}$-A] + KalTA4 RNA	41	30 (73.17%)***	26 (63.41%)***	21 (51.22%)***	24 (58.54%)***

Table S7 Summary of morphological phenotypes of *UAS-TdTom-miR-shRNA1$^{apkc\lambda}$*-A transgenic lines injected with *Pef1α-GFF* plasmid. ***: *P*< 0.001, vs Sibling + *Pef1α-GFF* plasmid.

	Number of embryos	Embryos with defective heart tube	Embryos with abnormal body curvature	Embryos with patchy RPE	Embryos with abnormally narrow brain ventricle
Sibling + *Pef1α-GFF* plasmid	43	2 (4.65%)	3 (6.98%)	0 (0.00%)	1 (2.33%)
Tg[UAS-TdTom-miR-shRNA1$^{apkc\lambda}$-A] + Pef1α-GFF plasmid	40	28 (70.00%)***	29 (72.50%)***	23 (57.50) ***	21 (52.50%)***